Centrum voor Wiskunde en Informatica
REPORT*RAPPORT*

A basic mathematical and numerical model for gas injection

J. Molenaar

Department of Analysis, Algebra and Geometry

AM-R9610 July 31, 1996

Report AM-R9610
ISSN 0924-2953

CWI
P.O. Box 94079
1090 GB Amsterdam
The Netherlands

A Basic Mathematical and Numerical Model for Gas Injection

J. Molenaar

CWI

P.O. Box 94079, 1090 GB Amsterdam, The Netherlands

Abstract

In this paper we discuss a mathematical model for gas storage processes. In addition we outline an approach for numerical simulations. The focus is on model assumptions and limitations with respect to the software to be developed.

AMS Subject Classification (1991): 65M06, 76S05

Keywords & Phrases: second-order accurate discretizations, gas storage

1. Introduction

Gas injection into gas reservoirs can be considered for reasons of gas storage or CO_2 disposal. It is the purpose of this paper to present a basic mathematical model for these gas injection processes, and to outline a numerical approach. Since we aim at developing numerical software, we focus on the model assumptions and limitations (Section 2). The mathematical model used (Section 3) is quite standard, and is discussed in more detail in [2] and [3]. In addition to the mathematical model we outline the numerical method to be used (Section 4). After discussing the concept of numerical diffusion, we propose a method that should minimize the detrimental effects of numerical diffusion. To demonstrate the soundness of our approach, we show computational results for a simple linear model problem, and a more realistic problem describing a cycle of gas storage.

2. Model Assumptions

Major assumptions in our mathematical model for gas injection are

A1. The gas consists of two pseudo-components with different viscosity and density.

A2. The flow is two-dimensional.

A3. Darcy's law is valid.

A4. The microscopic mixing is caused by molecular diffusion and convective dispersion. The mixing is described by Fick's first law.

A5. No-flow conditions are prescribed at the domain boundary.

A6. Gravity effects are negligible.

A7. The rock permeability is described by a diagonal tensor.

A8. Rock compressibility is negligible.

A9. Wells are modeled by point sources. At a well either the flow rate is prescribed, or the pressure.

A10. The reservoir temperature is uniform and constant.

A11. The density and viscosity of the gas in the mixing zone are given functions of the pressure and gas composition only.

Apart from these physical assumptions there is an additional assumptions that we use in the numerical algorithm:

A12. The domain is decomposable into rectangles, so orthogonal grids can be used.

3. Mathematical Model

3.1 Choice of variables

The composition of the gas mixture is defined in terms of a mole fraction. The mole fraction y_i of pseudo-component i is defined by

$$y_i = \frac{c_i}{C}, \tag{3.1}$$

where c_i is the molar concentration of pseudo-component i (the number of moles of pseudo-component i per unit volume), and C the total molar concentration,

$$C = c_1 + c_2, \tag{3.2}$$

so

$$y_1 + y_2 = 1. \tag{3.3}$$

We use two independent variables: the gas pressure P and the mole fraction y_1 of pseudo-component 1. The reason for using the mole fraction as the independent variable, instead of the mass concentration (mass per unit volume), is that we expect that the total molar concentration is a smoother function than the total mass density.

3.2 Flow Equations

The total volumetric flow rate $\mathbf{u}$ of gas is determined by Darcy's law (**A**3,**A**6):

$$\mathbf{u} = -\frac{1}{\mu} K \cdot \nabla P, \tag{3.4}$$

where K is the diagonal permeability tensor (**A**7), and μ the viscosity of the mixture. The total molar flux (number of moles per unit area per unit time) is given by

$$\mathbf{j} = C\mathbf{u}. \tag{3.5}$$

The molar flux $\mathbf{j}_{d,i}$ of pseudo-component i due to diffusion and dispersion is described by Fick's law (**A**4) (see [1]):

$$\mathbf{j}_{d,i} = -CD \cdot \nabla y_i. \tag{3.6}$$

The dispersion tensor D is in two space dimensions defined by

$$D = \alpha_m I + \frac{\alpha_l}{|\mathbf{j}|} \begin{pmatrix} j_x^2 & j_x j_y \\ j_x j_y & j_y^2 \end{pmatrix} + \frac{\alpha_t}{|\mathbf{j}|} \begin{pmatrix} j_y^2 & -j_x j_y \\ -j_x j_y & j_x^2 \end{pmatrix}, \tag{3.7}$$

where α_m, α_l and α_t represent molecular diffusion, longitudinal dispersion and transversal dispersion, respectively.

The molar flux of each pseudo-component consists of two terms, a convective term and a dispersion term. Hence for both pseudo-components we have the following molar conservation laws:

$$\phi \frac{\partial y_i C}{\partial t} + \nabla \cdot (y_i \mathbf{j} - CD \cdot \nabla y_i) = q_i, \quad i = 1, 2, \tag{3.8}$$

where q_i denotes the injection rate for pseudo-component i in moles per unit time per unit volume. Summing these two equations and using (3.3) gives

$$\phi \frac{\partial C}{\partial t} + \nabla \cdot \mathbf{j} = q_1 + q_2 = Q, \tag{3.9}$$

where Q denotes the total injection rate. Substitution of Darcy's law (3.4) and (3.5) yields the pressure equation:

$$\phi \frac{\partial C}{\partial t} - \nabla \cdot \left(\frac{C}{\mu} K \cdot \nabla P \right) = Q. \tag{3.10}$$

This pressure equation combined with the the molar conservation law (3.8) for component 1 form the system of partial differential equations that describe the problem. Both the viscosity μ and the total molar concentration C depend on the pressure P and the gas composition y_1. Usually it is assumed that the gas composition is constant. In that case the pressure equation can be made 'more linear' by introducing a pseudo-pressure variable. Because we are dealing with cases that the composition of the gas varies through the reservoir, we cannot use a pseudo-pressure variable.

3.3 Boundary Conditions

There are only no-flow boundary conditions (**A**5).

3.4 Wells

At wells either the flow rate is prescribed, or the pressure. The volumetric flow rate (at reservoir conditions) into a well for given bottom hole flowing pressure P_{wf} is

$$u = \frac{2\pi K h}{\mu \left(\log(r_e/r_w) - 1/2 + S \right)} (P - P_{wf}), \tag{3.11}$$

where h denotes the thickness of the reservoir, r_w and r_e the well and drainage boundary radius, respectively, and S the so called skin factor.

3.5 Mixing Rules

The molar concentration of a real gas is given by

$$C = \frac{P}{zRT}, \tag{3.12}$$

where R is the gas constant, T the temperature and z the Z-factor that describes the deviation from the ideal gas law.

The Z-factor is an empirical factor that can be determined by the following method proposed by Hall and Yarborough [4]. Let P_{ci} and T_{ci} be the critical pressure and temperature of pseudo-component i. The reduced pressure and temperature are defined by

$$P_r = \frac{P}{y_1 P_{c1} + y_2 P_{c2}}, \tag{3.13}$$

$$T_r = \frac{T}{y_1 T_{c1} + y_2 T_{c2}}. \tag{3.14}$$

The Z-factors are then implicitly given by

$$a + \frac{Y + Y^2 + Y^3 - Y^4}{(1-Y)^3} - bY^2 + cY^d = 0, \tag{3.15}$$

where

$$a = -0.06125(P_r/T_r)\exp\left(-1.2(1-1/T_r)^2\right) \tag{3.16}$$

$$b = 14.76T_r^{-1} - 9.76T_r^{-2} + 4.58T_r^{-3}, \tag{3.17}$$

$$c = 90.7T_r^{-1} - 242.2T_r^{-2} + 42.4T_r^{-3}, \tag{3.18}$$

$$d = 2.18 + 2.82T_r^{-1}, \tag{3.19}$$

$$Y = -a/z. \tag{3.20}$$

Because the reservoir temperature is constant (**A**10), relation (3.15) implicitly defines the Z-factor as a function of the reduced pressure P_r.

The gas viscosity can be determined from the model proposed by Lee e.a. [5] (**A**11):

$$\mu = K\exp(X(10^{-3}\rho)^Y), \tag{3.21}$$

where

$$K = \frac{(22.7 + 48M)T^{1.5}}{209 + 19000M + 1.8T}, \tag{3.22}$$

$$X = 3.5 + 548/T + 10M, \tag{3.23}$$

$$Y = 2.4 - 0.2X. \tag{3.24}$$

Another possible model for the viscosity is given by Lohrenz e.a. [6].

Here we have summarized two popular models for the density and viscosity, but more mixing rules can be found in the literature. For our purposes it is sufficient to assume that the density and viscosity are given functions of the pressure P and the composition y_i.

4. Numerical Method

In this section we first discuss the concept of numerical diffusion in standard first-order accurate schemes for the linear convection equation. To minimize the amount of numerical diffusion we propose to use second-order accurate schemes. The feasibility of this approach is shown by comparing the numerical solutions for the radial convection-diffusion equation. Next we present a discretization for the full model: we extend the approach outlined in Section 4.1 to the pressure equation (3.10) and the transport equation (3.8). A numerical experiment with a single cycle of gas storage again shows the merits of the second-order accurate schemes, although there is room for improvement.

4.1 Numerical diffusion

The concept of numerical diffusion is based on the study of the one-dimensional convection equation

$$\frac{\partial c}{\partial t} + u\frac{\partial c}{\partial x} = 0. \tag{4.25}$$

Let us consider the standard forward in time and upwind in space scheme for $u > 0$,

$$c_i^{n+1} = (1-\lambda)c_i^n + \lambda c_{i-1}^n, \tag{4.26}$$

where the subscript i denotes the discretization cell, the superscript n the time step and λ the so-called CFL-number that is defined by

$$\lambda = u\frac{\Delta t}{\Delta x}. \tag{4.27}$$

The truncation error of this discretization is found by substituting the exact solution of (4.25) into the discrete equation (4.26). Substituting the Taylor expansions of the solution $c(x,t)$ of (4.25) around (x_i, t^n)

$$c(x_{i-1}, t^n) = c(x_i, t^n) - \Delta x\frac{\partial c}{\partial x}(x_i, t^n) + \frac{1}{2}\Delta x^2\frac{\partial^2 c}{\partial x^2}(x_i, t^n) + \mathcal{O}(\Delta x^3), \tag{4.28}$$

$$c(x_i, t^{n+1}) = c(x_i, t^n) + \Delta t\frac{\partial c}{\partial t}(x_i, t^n) + \frac{1}{2}u^2\Delta t^2\frac{\partial^2 c}{\partial x^2}(x_i, t^n) + \mathcal{O}(\Delta x^3), \tag{4.29}$$

into (4.26) yields

$$\frac{\partial c}{\partial t}(x_i, t^n) + u\frac{\partial c}{\partial x}(x_i, t^n) = \frac{u}{2}(1-\lambda)\Delta x\frac{\partial^2 c}{\partial x^2}(x_i, t^n). \tag{4.30}$$

Clearly the exact solution of (4.25) does not satisfy the discrete equation (4.26). Conversely, the solution to the discrete equation (4.26) does not satisfy (4.25), but the modified differential equation (4.30) with the extra (numerical) diffusion term

$$\frac{u}{2}(1-\lambda)\Delta x\frac{\partial^2 c}{\partial x^2}. \tag{4.31}$$

For $\lambda = 1$ this numerical diffusion term vanishes, and for $\lambda > 1$ the anti-diffusion term causes numerical instability.

The modified equation (4.30) shows that the additional diffusion term vanishes as $\mathcal{O}(\Delta x)$ for $\Delta x \to 0$. This term appears because both the upwind in space and the forward in time

$\psi(r)$	
$\min(1, r + \|r\|)$	Davis
$\max(0, \min(2, 2r, (2r+1)/3))$	Leonard
$(r + \|r\|)/(1 + r)$	Van Leer
$(r^2 + r)/(r^2 + 1)$	Van Albada

Table 4.1: Overview of some popular limiter functions $\psi(r)$.

discretization are only first-order accurate. Of course one can try to balance these two contributions to the numerical diffusion by taking $\lambda \approx 1$. However, for our problem we expect a radial velocity field (**A**9). Because the velocity field is not uniform is seems impossible to have $\lambda \approx 1$ throughout the domain. Moreover the use of the explicit Euler scheme for the time integration in (4.26) enforces a small time step, because the velocities near the well are very high. Violating the CFL-condition $\lambda \leq 1$ leads to numerical instability.

A systematic way to decrease the numerical diffusion is to use a scheme that is more accurate with respect to the discretization in both space and time. Therefore we consider cell-centered discretizations of (4.25) of the form

$$\frac{d\,c_i}{d\,t} = -u\frac{c_{i+1/2} - c_{i-1/2}}{\Delta x}, \tag{4.32}$$

where $c_{i+1/2}$ is an approximation of c at the edge between the cells i and $i+1$. In the first-order upwind scheme $c_{i+1/2}$ is approximated by c_i. More accurate discretizations are obtained by using a larger stencil. A rather general class of schemes are the so-called κ-schemes that are generated by

$$c_{i+1/2} = c_i + \frac{1+\kappa}{4}(c_{i+1} - c_i) + \frac{1-\kappa}{4}(c_i - c_{i-1}), \quad \kappa \in [-1, +1]. \tag{4.33}$$

For $\kappa = -1$ we obtain the two-point upstream scheme, and for $\kappa = +1$ the central discretization. All these κ-schemes suffer from 'wiggles' near strong gradients in the solution. (In fact, these problems are caused by the lack of numerical diffusion.) To avoid these wiggles the scheme is changed: where the solution is smooth we use (4.33), but near strong gradients we switch over to a scheme that introduces more numerical diffusion. The smoothness of the solution is measured by the ratio of consecutive gradients r

$$r_{i+1/2} = \frac{c_{i+1} - c_i}{c_i - c_{i-1}}, \tag{4.34}$$

so if the solution is locally smooth we have $r \approx 1$. We now approximate $c_{i+1/2}$ as follows:

$$c_{i+1/2} = c_i + \frac{1}{2}\psi(r_{i+1/2})(c_i - c_{i-1}). \tag{4.35}$$

For second-order accuracy it is necessary that $\psi(1) = 1$. To suppress spurious wiggles restrictions are imposed on the function $\psi(r)$ (see e.g. [8]). An enormous amount of limiter functions have been proposed in the literature. Some of them are listed in Table 4.1.

The fact that $\psi(1) = 1$ does not mean that the scheme (4.35) is equivalent to a two-point upstream scheme, i.e., the scheme obtained by taking $\kappa = -1$ in (4.33). A careful analysis shows that in smooth parts of the solution, where $r \approx 1$, the limited schemes (4.35) are related to the κ-schemes (4.33) by

$$\psi'(1) = \frac{\kappa + 1}{2}. \tag{4.36}$$

It is important to note that the introduction of the limiter function leads to a nonlinear discrete scheme for the linear equation (4.25).

The proper choice of a time integration scheme for the system of ordinary differential equations (4.32) is difficult. There exists an enormous literature on schemes that are at least second order accurate. An important division in these schemes is whether they are implicit or explicit. Explicit schemes are computationally cheap per time step, but usually have to satisfy some time step criterion for stability reasons. Implicit schemes are more stable, but in each time step we have to solve large, possibly nonlinear systems of algebraic equations.

The transport equation, that we are eventually interested in, is of convection-diffusion type,

$$\frac{\partial c}{\partial t} = -u\frac{\partial c}{\partial x} + D\frac{\partial^2 c}{\partial x^2}. \tag{4.37}$$

The diffusion part of the operator necessitates an implicit scheme. A possible approach here is operator splitting. An explicit scheme is then used is used for the time integration of the convective part of the operator, and an implicit scheme for the diffusive part. This splitting is quite tricky, and a possible source of instability. Moreover, because we have to deal with radial velocity fields (**A**9), the stability conditions for explicit schemes may turn out to be too restrictive in practice.

Therefore we consider the use of implicit schemes. The backward Euler scheme,

$$c_i^{n+1} = c_i^n - \lambda(c_{i+1/2}^{n+1} - c_{i-1/2}^{n+1}), \tag{4.38}$$

is widely used, but it is inappropriate for our purposes because it is only first order accurate. The Crank-Nicholson scheme is an example of an implicit second-order accurate scheme:

$$c_i^{n+1} = c_i^n - \lambda\left(\frac{c_{i+1/2}^{n+1} + c_{i+1/2}^n}{2} - \frac{c_{i-1/2}^{n+1} + c_{i-1/2}^n}{2}\right). \tag{4.39}$$

Implicit schemes with even higher orders of accuracy are found in the class of implicit Runge-Kutta schemes. However, since we aim at second-order accuracy we propose to use the Crank-Nicholson scheme.

4.2 Numerical example I

To compare some of the schemes that we have discussed, we consider the two-dimensional radial convection-diffusion equation,

$$\frac{\partial c}{\partial t} + \frac{q}{h}\nabla \cdot c\frac{\hat{r}}{|r|} = \nabla \cdot (D \cdot \nabla c), \tag{4.40}$$

where q is the volumetric injection rate, h the thickness of the layer and r the radial vector. For the initial and boundary conditions

$$c(0,t) = 1, \tag{4.41}$$
$$c(\infty,t) = 0, \tag{4.42}$$
$$c(r,0) = 0 \tag{4.43}$$

and

$$h = 1, \tag{4.44}$$
$$q = 2\pi \tag{4.45}$$

the exact solution is given by

$$c(r,t) = \Gamma\left(\frac{1}{2D}, \frac{|r|^2}{4Dt}\right), \tag{4.46}$$

where $\Gamma(\cdot,\cdot)$ is the (normed) incomplete gamma-function. We discretize this problem on a unit square, and put the injection point in a corner of the unit square. For small values of t and D the influence of the finiteness of the domain is negligible. In our numerical experiment we take $\alpha_m = 0.05$ and $t = 0.15$. A contour plot of the exact solution is shown in Figure 4.1. The contour lines are drawn at $c = 0.1, 0.2, \cdots, 0.9$. We compare the following schemes:

S1T1E The backward in space and forward in time scheme (4.26), which is explicit and first-order accurate in both space and time,

S2T2E The second-order accurate in space scheme (4.35) with an explicit second-order accurate time integration,

S2T2I The second-order accurate in space and time scheme (4.35,4.39), which is implicit. The discrete problem in each time step is solved by a multigrid method (see [7]).

For the second-order accurate in space discretizations we use the Van Leer limiter (see Table 4.1). In the implicit scheme S2T2I we adaptively determine the time step, so that

$$\max_{i,j} |c_{i,j}^{n+1} - c_{i,j}^{n}| \approx 0.05. \tag{4.47}$$

This means that the time step increases during the simulation, since the movement of the front slows down. This approach fails for the explicit schemes S1T1E and S2T2E, because too large time steps lead to numerical instability. For the explicit schemes we use a fixed time step that is determined by the condition $\lambda_{\max} < 0.5$.

In Table 4.2 the results are shown for calculations on different grids. The grid ℓ_2-error at $t = 0.15$ of the numerical solution clearly exhibits the difference in convergence behavior for the different schemes. Halving of the mesh width reduces the error by a factor of approximately 0.5 for the first order method S1T1E, whereas the error is reduced by a factor 0.25 for the second order methods S2T2E and S2T2I. Although the computing time needed depends on many factors (implementation, computer architecture, specific problem, etc.), comparison of the results in Table 4.2 reveals a clear trend. The number of time steps needed for the explicit

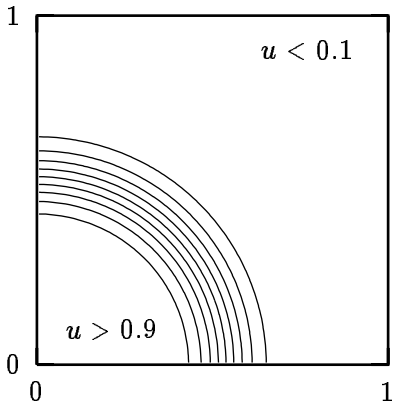

Figure 4.1: Contour plot of the solution of the radial convection-diffusion equation at $t = 0.15$.

		20×20	40×40	80×80
ℓ_2-error	S1T1E	.0400	.0230	.01200
	S2T2E	.0062	.0015	.00034
	S2T2I	.0060	.0013	.00024
CPU time [sec]	S1T1E	4	57	927
	S2T2E	11	176	2942
	S2T2I	12	66	394
number of steps	S1T1E	771	3033	12080
	S2T2E	771	3033	12080
	S2T2I	105	141	177
time per step [sec]	S1T1E	0.005	0.019	0.077
	S2T2E	0.014	0.058	0.244
	S2T2I	0.114	0.468	2.226

Table 4.2: Numerical results for the radial convection-diffusion equation.

methods grows as h^{-2}. This is due to the fact that the maximum velocity in the discretized problem grows as h^{-1}. Because the amount of work per time step grows as h^{-2}, the total amount of work for the whole computation grows as h^{-4}. We expect that the number of time steps needed in the implicit method, where the time step is chosen adaptively, grows as h^{-1}. In our numerical example the growth rate is even less. Therefore the total time needed grows at most as fast as h^{-3}. We generally expect this type of behavior for radial velocity fields.

4.3 Discretization

Let us now consider the discretization of our full model (3.4-3.10)

$$\mathbf{j} = -\frac{C}{\mu} K \cdot \nabla P, \tag{4.48}$$

$$\phi \frac{\partial C}{\partial t} + \nabla \cdot \mathbf{j} = Q, \tag{4.49}$$

$$\phi \frac{\partial yC}{\partial t} + \nabla \cdot (y\mathbf{j} - C\,D \cdot \nabla y) = q, \tag{4.50}$$

where we have dropped the subscript 1 on y and q. At the heart of our discretization is the assumption that the pressure P is a smooth variable, whereas the mole fraction y can be discontinuous. As in Section 4.1 we split the time and space discretization. For the space discretization we use a cell-centered finite difference scheme. Because we have orthogonal grids (**A**12), it suffices to consider the one-dimensional case. For ease of notation we restrict ourselves to uniform meshes. The space discretized conservation equations are then

$$Q_i = \phi \frac{d\,C_i}{d\,t} + \frac{j_{i+1/2} - j_{i-1/2}}{\Delta x}, \tag{4.51}$$

$$\begin{aligned} q_i = \phi \frac{d\,y_i C_i}{d\,t} &+ \frac{y_{i+1/2} j_{i+1/2} - y_{i-1/2} j_{i-1/2}}{\Delta x} \\ &- D_{i+1/2} C_{i+1/2} \frac{y_{i+1} - y_i}{\Delta x^2} + D_{i-1/2} C_{i-1/2} \frac{y_i - y_{i-1}}{\Delta x^2}. \end{aligned} \tag{4.52}$$

The quantities at the cell edge $i + 1/2$ are approximated by

$$j_{i+1/2} = -\frac{C_{i+1/2}}{\mu_{i+1/2}} K_{i+1/2} \frac{P_{i+1} - P_i}{\Delta x}, \tag{4.53}$$

$$C_{i+1/2} = C(y_{i+1/2}, P_{i+1/2}), \tag{4.54}$$

$$\mu_{i+1/2} = \mu(y_{i+1/2}, P_{i+1/2}), \tag{4.55}$$

$$P_{i+1/2} = \frac{P_{i+1} + P_i}{2} \tag{4.56}$$

and

$$y_{i+1/2} = \begin{cases} y_i + \frac{1}{2}\psi(r_{i+1/2})(y_i - y_{i-1}) & \text{if } j_{i+1/2} \geq 0, \\ y_{i+1} - \frac{1}{2}\psi(1/r_{i+3/2})(y_{i+2} - y_{i+1}) & \text{if } j_{i+1/2} < 0. \end{cases} \tag{4.57}$$

Notice that we use simple averaging to approximate $P_{i+1/2}$, and an upwind weighted approximation for $y_{i+1/2}$. The standard first order upwind scheme is retained by taking $\psi \equiv 0$.

grid	S1T1I	S2T2I
10×10	0.152	0.071
20×20	0.120	0.043
40×40	0.086	0.020
80×80	0.070	0.014
160×160	0.044	0.010

Table 4.3: Amount of unphysical mixing for simple gas injection problem.

4.4 Numerical Example II

To assess the merits of this discretization we consider a simple gas storage problem. The reservoir is a square with a side length of 200 m and a thickness of 20 m. The reservoir has a uniform porosity and permeability ($\phi = 0.2$ and $K = 50$mD), and the reservoir temperature is 70 °C. Initially the reservoir is filled with gas 1 at a pressure of 35 bar, and during 150 days gas 2 is injected into the reservoir with an injection rate of $30 \cdot 10^3\,\mathrm{Nm}^3/\mathrm{d}$. The well is located in a corner of the reservoir. During the next 150 days gas is withdrawn from the reservoir with a fixed withdrawal rate of $30 \cdot 10^3\,\mathrm{Nm}^3/\mathrm{d}$. For simplicity we assume that both gases can be treated as ideal gases, and that their viscosities are equal and constant. For all relevant gas data we take the properties of methane. Because there is no physical dispersion in the problem, we expect a sharp interface between gas 1 and 2.

We compute the solution to this problem with two different schemes, that are labeled by

S1T1I The backward in space ($\psi \equiv 0$) and time scheme (4.38), which is implicit and first order accurate in both space and time,

S2T2I The second order accurate in space and time scheme (4.39), which is also implicit.

In Table 4.3 the amount of unphysical mixing is shown, that is the ratio of the amount of the initially present gas 1 that is produced, and the total amount of gas produced. Two conclusion can be drawn from these results. First, we observe that the second-order accurate scheme S2T2I indeed introduces much less unphysical mixing than the first-order accurate scheme S1T1I. Second, we see that the the formally second-order accurate scheme S2T2I has a lower order of accuracy for this problem: it appears to be only first order accurate. The reason for this loss of accuracy is the following. In the problem there is no diffusion or dispersion. That means that the interface between the two gases is sharp. Near discontinuities the limiter function ψ locally causes a switch to a first-order accurate discretization. In the numerical solution the discontinuity is smeared out over a fixed number of grid points. That means that the scheme is only first-order accurate with respect to the amount of gas 1 that is being produced.

5. Conclusion

We propose to use a method like S2T2I, that is implicit and second order accurate in both space and time. The advantage of such methods is that the amount of numerical diffusion is much less than in conventional first order accurate methods. If the amount of physical mixing is not negligible, the results for the radial convection-diffusion equation show the superior

convergence behavior of second-order accurate methods compared with first-order methods. But if the amount of physical mixing is small, and the mixing zone cannot be properly represented on a fine grid, the method S2T2I is no longer second-order accurate, although it still outperforms the first-order method. However, the second-order accurate methods appear to be a good candidate, because we expect that the problems of interest display an appreciable amount of physical mixing.

References

1. R.B. Bird, W.E. Stewart, and E.N. Lightfoot. *Transport Phenomena.* John Wiley, 1960.
2. L.P. Dake. *Fundamentals of reservoir engineering.* Elsevier, 1978.
3. J. Hagoort. *Fundamentals of Gas Reservoir Engineering*, volume 23 of *Developments in Petroleum Science.* Elsevier, 1988.
4. K.R. Hall and L. Yarborough. A new equation-of-state for z-factor calculations. In *Gas Technology*, volume 13 of *SPE reprint series.* SPE, 1977.
5. A.L. Lee, M.H. Gonzalez, and B.E. Eakin. The viscosity of natural gases. In *Gas Technology*, volume 13 of *SPE reprint series.* SPE, 1977.
6. J. Lohrenz, B.G. Bray, and C.R. Clark. Calculating viscosities of reservoir fluids from their composition. In *Gas Technology*, volume 13 of *SPE reprint series.* SPE, 1977.
7. J. Molenaar. Multigrid methods for fully implicit oil reservoir simulation. Technical Report 95-40, T.U. Delft, 1995. To appear in "Proceedings Copper Mountain Conference on Multigrid Methods 1995".
8. P.K. Sweby. High resolution schemes using flux limiters for hyperbolic conservation laws. *SIAM J. Numer. Anal.*, 21:995–1011, 1984.